The effect of Tri- and Tetra-vacancies defects on the electronic and vibrational properties of (14, 5) chiral carbon nanotube

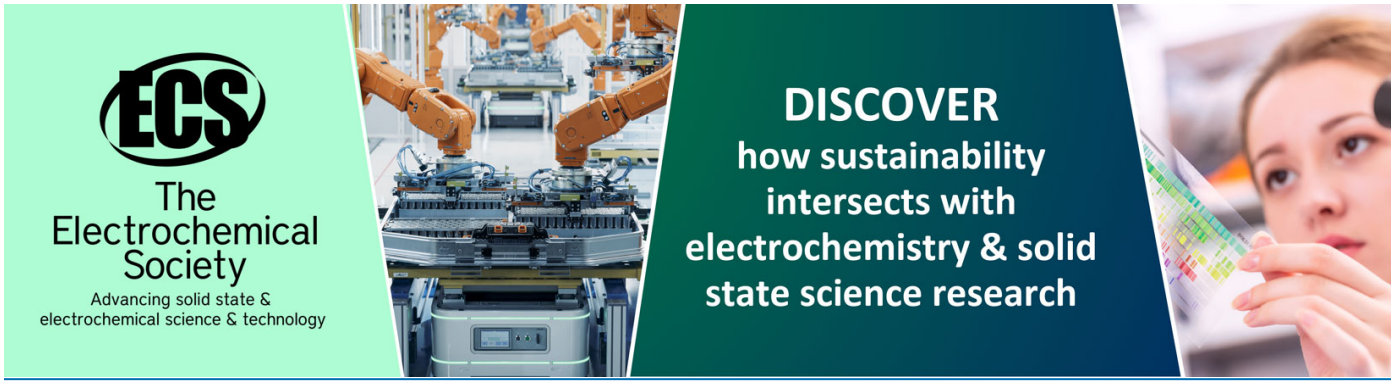

IOP Conf. Series: Materials Science and Engineering **783** (2020) 012018 doi:10.1088/1757-899X/783/1/012018

The effect of Tri- and Tetra-vacancies defects on the electronic and vibrational properties of (14, 5) chiral carbon nanotube

SA Ait Abdelkader, M Boutahir, AH Rahmani, B Fakrach, M Bentaleb, H Chadli and A Rahmani

Advanced Material and Applications Laboratory (LEM2A), University Moulay Ismail,FSM-ESTM-FPE, BP 11201, Zitoune, 50000 Meknes, Morocco.

E-mail: a.rahmani@fs-umi.ac.ma

Abstract. In this theoretical work, using the spectral moment's method and the bond polarisability model, the non-resonant Raman spectra of (14,5) chiral carbon nanotube with Tri- and Tetra-vacancies defects were calculated. The evolution of the Raman lines of defectives CNTs as a function of the defects concentration was discussed. It is observed that, the Raman spectra of defective carbon nanotubes present the D-band around 1350 cm-1. The Raman characteristics modes of TriV and TetraV defects are identified. The evolution of the electronic density of states as a function of the defects concentration was investigated. This study can provide benchmark to understand the experimental data of defective CNTs.

1. Introduction

Carbon nanotubes [1] and graphene [2] have been extensively studied [3, 4, 5, 6]] given to their exceptional structural, mechanical and electronic properties [7, 8, 9, 10, 11], and are widely used in several applications including electronics, charge transport and biomedical sensing [12, 13]. In practice, it is almost impossible to work with defect-free materials, and some structural point's defects can be introduced unintentionally during the growth [14] or under electron irradiation [15] and chemical treatments. Since the synthetized materials are usually not ideal crystal, the properties mentioned above can be significantly altered due to some unavoidable structural point's defects during the synthesis processes. Several kinds of points defects can be sited in the wall of the synthetized carbon nanotubes [16, 17], such as Stone-Wales defects [18, 19], ad-atoms [20, 21] and vacancies [22, 23, 24]. Among them, the vacancies are the most prolific and important defects, because they certainly have an influence on the mechanical, physical and chemical properties of carbon nanotubes. Therefore, it is very important to understand how the vacancies defects tailor the intrinsic properties of this system. Great attention has been focused on the study of atomic vacancies effect on the carbon nanotube properties [25, 26, 27]. It has been found that the tensile strength and critical stress of carbon nanotubes decrease due to the mono-vacancies and small vacancy clusters [28, 29]. The dangling bonds generated by the vacancies in CNTs (Carbon Nanotubes) can act as active sites for adsorptions [30, 31]. Concerning the vacancies effect on the electronic properties of carbon nanotubes, it's found that the vacancies induced changes and create new available states at around Fermi level [32]. It's

estimated that the density of states around the Fermi level rises due to the broken ? bands at the vacancies site [33]. Raman spectroscopy is a characterization technique extremely sensitive to molecules geometries and the bondings between their atoms. This sensitivity is extremely useful for the study of the different carbon allotropes (i.e. carbon nanotubes, fullerenes, graphene, etc.). The Raman spectrum of perfect carbon nanotube is dominated by the so-called RBM (Radial Breathing Mode) band below 350 cm^{-1} and by the G band in the high wave number region. It was found that the RBM mode directly related to the tube diameter [34], and it can be used to estimate the distribution of tube diameters in samples [35]. The G-band is due to the vibration of carbon atoms in plane involving the tube wall. Usually, another mode is observed at around 1350 cm^{-1}. This mode is known by the D-band and is a defect signature in the graphene lattice and is often used to characterize defective carbon nanotubes. This paper discusses the effect of Tri- and Tetra-vacancies defect on the vibrational and electronic properties of (14,5) chiral carbon nanotube and provides an updated overview of the current characterization tools able to identify and detect vacancies-defects in carbon nanotubes.

2. Computational method

We focus on the electronic and the vibrational properties of Tri- and Tetra-vacancies defect in (14,5) chiral carbon nanotube (Figure 1). We use the Raman spectroscopy, such as a perfect tool to get important information and characterization of both perfect and defective carbon nanotube.

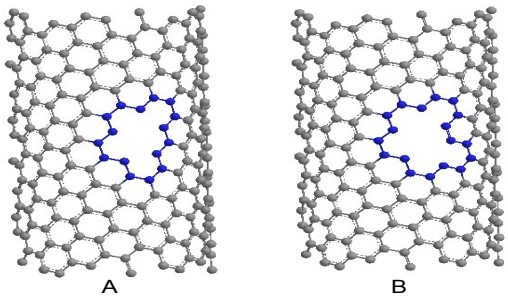

Figure 1. Molecular models of carbon nanotube with Tri- vacancy defect (A) and Tetra-vacancy defects (B).

For this purpose, by using the force constant model introduced by Wirtz and Rubio [36], we described the C-C interactions of the carbon atoms sited on the perfect area between vacancies defects. The interactions C-C of carbon atoms surounding the vacancies defects are calculated by using Density Functional Theory (DFT) as implemented inside the SIESTA package [**?**].

The Raman intensity is obtained according to the bond polarizability model [**?**]. In this approach, the polarization is just modulated for the nearest-neighbor bonds and the components of the induced polarizability tensor are given by the empiric equation:

$$\pi_{\alpha\beta}(r) = \frac{1}{3}(\alpha_l + 2\alpha_p)\delta_{\alpha\beta} + (\alpha_l - \alpha_p)\left(\hat{r_\alpha}\hat{r_\beta} - \frac{1}{3}\delta_{\alpha\beta}\right) \quad (1)$$

where α and β relate to the cartesian components (x,y,z) and $\overrightarrow{\hat{r}}$ is the unit vector along the vector $\vec{r}$ connecting atom n and atom m which are covalently bonded. The parameters α_l and α_p correspond to the longitudinal and perpendicular bond polarizability respectively. In this approximation, one can assume that the bond polarizability parameters are depending on the

bond lengths r only. The derivatives $\pi^n_{\alpha\beta,\gamma}$ are given by:

$$\begin{aligned}\pi^n_{\alpha\beta,\gamma} &= \sum_m \frac{1}{3}(\alpha'_l + 2\alpha'_p)\delta_{\alpha\beta}\hat{r_\gamma} \\ &+(\alpha'_l - \alpha'_p)\left(\hat{r_\alpha}\hat{r_\beta} - \frac{1}{3}\delta_{\alpha\beta}\right)\hat{r_\gamma} \\ &+\frac{\alpha_l - \alpha_p}{r}(\delta_{\alpha\gamma}\hat{r_\beta} + \delta_{\beta\gamma}\hat{r_\alpha} - 2\hat{r_\alpha}\hat{r_\beta}\hat{r_\gamma})\end{aligned} \tag{2}$$

where $\alpha' = \left(\frac{\partial\alpha}{\partial r}\right)\Big|_{r=r_0}$ and r_0 is the equilibrium bond distance. The bond polarizability parameters are:

$$\overline{\alpha} = 2\alpha'_p + \alpha'_l, \quad \overline{\beta} = \alpha'_l + \alpha'_p, \quad and \quad \overline{\gamma} = \frac{\alpha_l - \alpha_p}{r} \tag{3}$$

3. Results and discussion

In this section, the effect of Tri- (Tetra-) vacancies on the vibrational and electronic properties of (14,5) chiral carbon nanotube is investigated. The defect concentration is defined as the report of the number of the removed atoms by the total number of atoms in the perfect tube.

3.1. Raman Spectra of Carbon Nanotubes with Tri- And Tetra-Vacancies Defects

We report the evolution of the Raman spectra of the defective (14,5) carbon nanotube as a function of the Tri- and Tetra-vacancies defect concentration. The vacancies concentration varied from 0% (for perfect tube) 1%, 2%, 3%, 4% and 5% (for the defective carbon nanotube). The studied samples are composed by a large number of carbon atoms (up to 24000 degrees of freedom). The maximum number of Tri- (Tetra-) vacancies defects can reach 1332 (1000) respectively. The nanotube axis is along the Z-axis. The laser beam is kept along the Y-axis of the reference frame. We consider that both incident and scattered polarizations are along the Z-axis to calculate the polarized ZZ spectra. The evolution of the obtained Raman spectra as function of tri-vacancies defect concentration are reported in the panels of Figure 2 with their corresponding pure nanotube (indicated by 0%). The spectra are displayed in the RBM (Radial Breathing Mode) range (left), intermediate range (middle), and the tangential modes range (right).

It is observed from the figure 2, that there is a significant effect of the Tri-vacancies defects on the Raman lines of the perfect tube. As we can see, the frequency of the RBM mode decreases as a function of the tri-vacancies concentration. When the concentration of tri-vacancies increases, the RBM downshifts from 166 cm^{-1} in pristine tube to 164 cm^{-1}, 163 cm^{-1}, 161 cm^{-1}, 159 cm^{-1}, 158 cm^{-1} for 1%, 2%, 3%, 4% and 5% of tri-vacancies concentration on the (14,5) SWNT (Single-Walled Carbon nanotubes), respectively. A second-lowest Raman-active peak located at around the value 450 cm^{-1} is observed in the case of defect tube only. In the intermediate range, the spectra of defectives nanotubes have shown the D band at around 1340 cm^{-1}, while no Raman line is expected for the perfect tube. This mode arises from tri-vacancies defect and its intensity depends on the defect concentration. Similarly to the previous calculations for SWNTs, the G-band located in the TM range is weakly downshift as a function of defect concentration. For instance, the G mode downshifts from 1591 cm^{-1} in the perfect nanotube to 1586 cm^{-1} in the 5% defective nanotube. The eigenvector displacement of the mode located around 450 cm^{-1} in spectra of SWNTs with Tri-vacancies defect, is given in Figure (3-A). These vectors allow us to identify the radial displacements of atoms belonging to the Tri-vacancy ring. This mode could be used as the intrinsic Raman signature of the Tri-vacancies defect sited in the carbon nanotube.

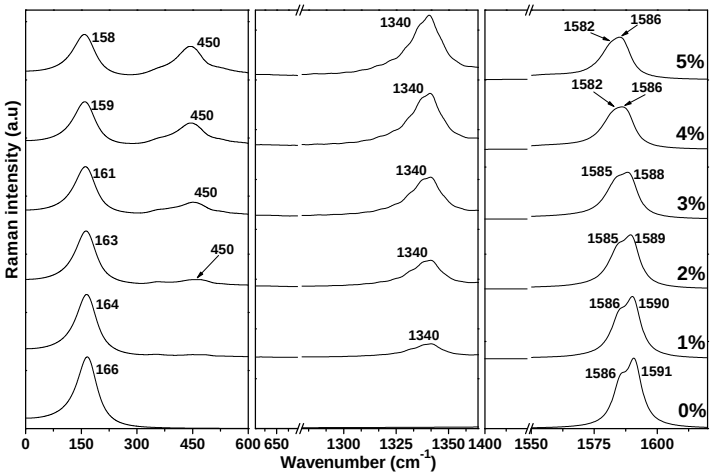

Figure 2. Evolution of the Raman spectra of (14,5) nanotube as a function of Tri-vacancies defects concentration.

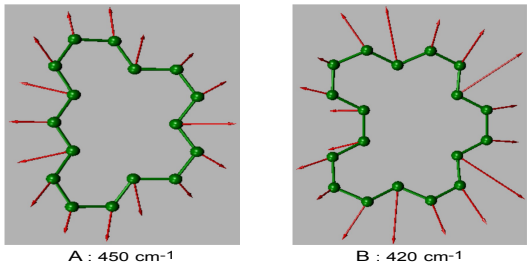

Figure 3. In A and B, the atomic displacements of Tri-vacancy and Tetra-vacancy in (14,5) nanotube, due to the Raman active modes at 450 cm^{-1} and 420 cm^{-1} respectively.

The Raman spectra of the chiral carbon nanotube (14.5) with Ttra-vacancy defects were calculated. The evolution of the obtained spectra as a function of the concentration of defects is illustrated in figure 4. As shown in the figure 4, the G mode (panel in the right) is slightly shifted to the low frequencies when the defect concentration increases. For example, the frequency of the G mode varies from 1591 cm^{-1} to the perfect nanotube (indicated by 0%) at 1586 cm^{-1} for the tube with 5% of Tetra-vacancies defects. In the intermediate zone, the spectra of the defective tubes have the D band around 1330 cm^{-1}. The eigenvector displacements of the mode around 420 cm^{-1} in the spectra of nanotubes with Tetra-vacancies defects are given in the figure (3-B). These vectors allow us to identify the radial displacements of atoms belonging to the Tetra-vacancy defect. In this mode, the atoms constituting the Tetra-vacancy ring moves in phase in the radial direction. This mode could be used as the Raman signature of the Tetra-vacancy sited in the carbon nanotube.

3.2. Band Structures and Density of States of Carbon Nanotubes with Tri- And Tetra-Vacancies Defects

Using the tight-binding model, the electronic bands structures and the electronic density of states of pristine and defective (14,5) carbon nanotube were calculated. These calculations were carried out for one unit cell of (14.5) tube (for pristine cell and defective cell with one and two

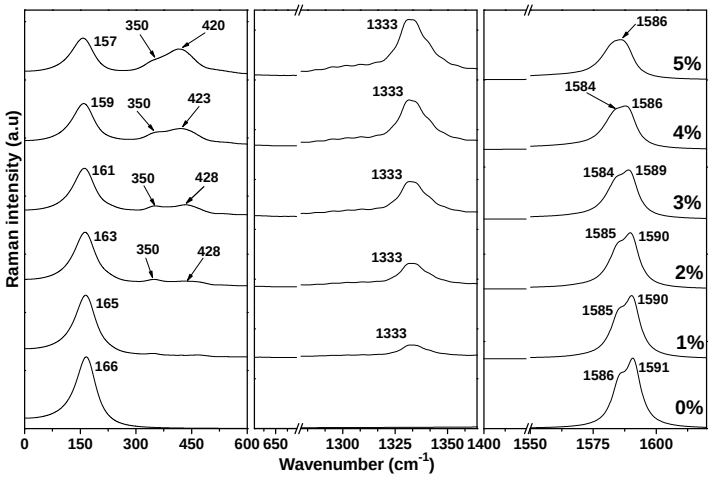

Figure 4. Evolution of the Raman spectra of (14,5) nanotube as a function of Tetra-vacancies defects concentration.

vacancies). The periodic conditions are applied along the axis of the tube. We present the obtained results in the direction ...M of the irreducible Brillouin zone of the structure of our system. The obtained bands structures and the densities of states of the (14, 5) tube with Tri- and Tetra-vacancies defects are shown in figures 5 and 6 respectively.

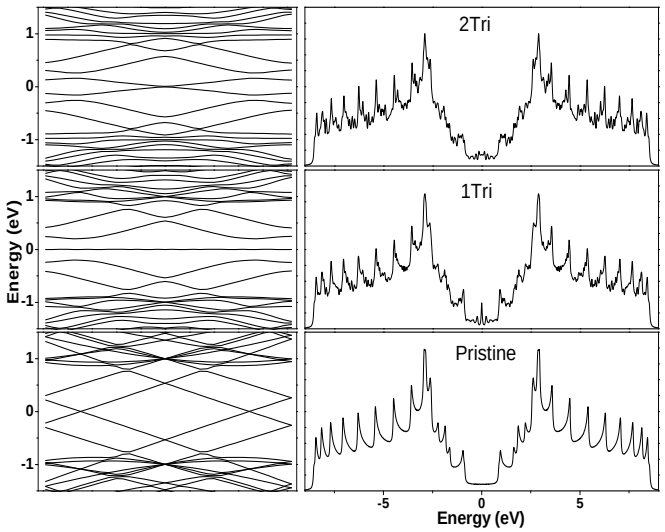

Figure 5. Band structure and density of states for (14,5) nanotube with Tri-vacancies defects.

In the case of Tri-vacancy defect in the (14.5) tube (Figure 5), we observe that there are new electronic states around the Fermi level. These electronics states are indicated by three peaks located around the Fermi level on the density of states of the tube with single Tri-vacancy (indicated by 1Tri). The first one is located at Fermi level (EF = 0 eV) and the two others are symmetric with respect to Fermi level. For the tube with two Tri-vacancies (2Tri), we observe that there are several new adjacent peaks. Concerning the Tetra-vacancy, we observe also that

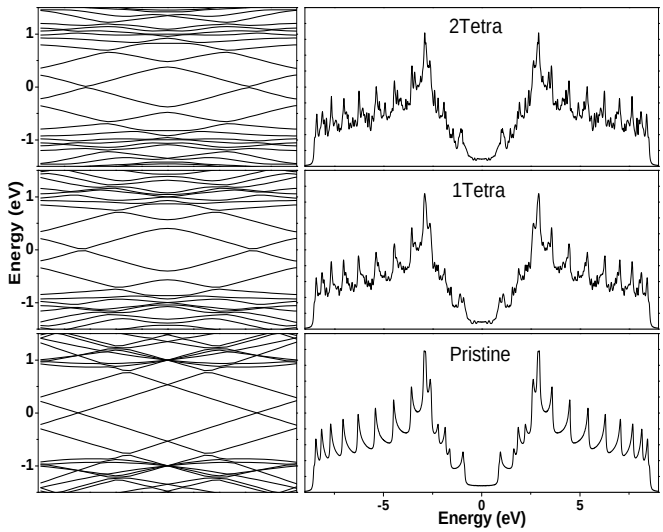

Figure 6. Band structure and density of states for (14,5) nanotube with Tetra-vacancies defects.

there are several new electronic states between the valence band and the conduction band. These new electronics states appeared like a several small peaks for the tube with one vacancy (two vacancies) as indicated respectively by 1Tetra (2Tetra) in figure 6. Such new electronics states could be due to the dangling bonds sited in the vacancies that introduced the localized empty defect states between the conduction band and valence band of the nanotube.

4. Conclusion

In this paper, the non-polarized Raman spectra of chiral (14,5) single-walled carbon nanotube with Tri- and Tetra-vacancies defects as a function of such defects concentration were investigated. Characteristic peaks of Tri- and Tetra-vacancies defects are identified in the radial breathing modes region. The obtained D band is in agreement with the experimental measurements. Using the tight-binding model, the electronic band structures and the density of states of (14,5) carbon nanotubes with the Tri- and Tetra-vacancies were also calculated. For the defective tubes, new electronic states around the Fermi level are identified.

Acknowledgments
The works was supported by a CNRST-Morocco agreement.

References

[1] S. Iijima 1991 Helical microtubules of graphitic carbon, nature 354 (6348) 56.
[2] K. S. Novoselov, A. K. Geim, S. V. Morozov, D. Jiang, Y. Zhang, S. V. Dubonos, I. V. Grigorieva, A. A. Firsov 2004 Electric field effect in atomically thin carbon films, science 306 (5696) 666-669.
[3] M. Boutahir, A. Rahmani, H. Chadli, A. Rahmani 2016 Mechanical coupled vibrations in an individual double-walled carbon nanotube, The European Physical Journal Applied Physics 74 (2) 24605.
[4] T. W. Odom, J.-L. Huang, P. Kim, C. M. Lieber 1998 Atomic structure and electronic properties of single-walled carbon nanotubes, Nature 391 (6662) 165 62.
[5] J. Mintmire, C. White 1995 Electronic and structural properties of carbon nanotubes, Carbon 33 (7) 893-902.
[6] M. Boutahir, A. Rahmani, B. Fakrach, H. Chadli, A. Rahmani 2016 Theoretical study of electronic and vibrational properties of dimer of single-wall carbon nanotubes, international journal of hydrogen energy 41 (45) 20874-20879

[7] I. Frank, D. M. Tanenbaum, A. M. van der Zande, P. L. McEuen 2007 Mechanical properties of suspended graphene sheets, Journal of Vacuum Science and Technology B: Microelectronics and Nanometer Structures Processing, Measurement, and Phenomena 25 (6) 2558-2561.
[8] S.-M. Choi, S.-H. Jhi, Y.-W. Son 2010 Effects of strain on electronic properties of graphene, Physical Review B 81 (8) 081407.
[9] J. N. Coleman, U. Khan, W. J. Blau, Y. K. Gunko 2006 Small but strong: a review of the mechanical properties of carbon nanotubepolymer composites, Carbon 44 (9) 1624-1652.
[10] T. Ando 2009 The electronic properties of graphene and carbon nanotubes, NPG asia materials 1 (1) 17.
[11] A. Jorio, G. Dresselhaus, M. S. Dresselhaus 2007 Carbon nanotubes: advanced topics in the synthesis, structure, properties and applications, Springer Science and Business Media Vol. 111, 185.
[12] G. Dresselhaus, S. Riichiro, et al. 1998 Physical properties of carbon nanotubes, World scientific.
[13] D. B. Mawhinney, V. Naumenko, A. Kuznetsova, J. T. Yates Jr, J. Liu, R. Smalley 2000 Surface defect site density on single walled carbon nanotubes 190 by titration, Chemical Physics Letters 324 (1-3) 213-216.
[14] J. A. Rodriguez-Manzo, F. Banhart 2009 Creation of individual vacancies in carbon nanotubes by using an electron beam of a diameter, Nano letters 9 (6) 2285-2289.
[15] T. Ebbesen, T. Takada 1995 Topological and sp3 defect structures in nanotubes, Carbon 195 33(7) 973-978.
[16] J.-C. Charlier 2002 Defects in carbon nanotubes, Accounts of chemical research 35 (12) 1063-1069.
[17] H. F. Bettinger 2005 The reactivity of defects at the sidewalls of single-walled carbon nanotubes: The stone-wales defect, The Journal of Physical Chemistry B 109 (15) 6922-6924.
[18] L. Zhou, S.-Q. Shi 2003 Formation energy of stone-wales defects in carbon nanotubes, Applied physics letters 83 (6) 1222-1224.
[19] P. G. Collins 2010 Defects and disorder in carbon nanotubes, Oxford Handbook of Nanoscience and Technology: Materials: Structures, Properties 205 and Characterization. Techniques 2 (2) 31.
[20] P. Lehtinen, A. S. Foster, A. Ayuela, A. Krasheninnikov, K. Nordlund, R. M. Nieminen 2003 Magnetic properties and diffusion of adatoms on a graphene sheet, Physical review letters 91 (1) 017202.
[21] S. Zhang, S. L. Mielke, R. Khare, D. Troya, R. S. Ruo, G. C. Schatz, 210 T. Belytschko 2005 Mechanics of defects in carbon nanotubes: atomistic and multiscale simulations, Physical Review B 71 (11) 115403.
[22] A. Hashimoto, K. Suenaga, A. Gloter, K. Urita, S. Iijima 2004 Direct evidence for atomic defects in graphene layers, Nature 430 (7002) 870.
[23] R. G. Amorim, A. Fazzio, A. Antonelli, F. D. Novaes, A. J. da Silva, 2007 Divacancies in graphene and carbon nanotubes, Nano Letters 7 (8) 2459-2462.
[24] M. Huhtala, A. Krasheninnikov, J. Aittoniemi, S. Stuart, K. Nordlund, K. Kaski 2004 Improved mechanical load transfer between shells of multiwalled carbon nanotubes, Physical Review B 70 (4) 045404.
[25] S. A. A. Abdelkader, F. Fergani, M. Bentaleb, M. Boutahir, B. Fakrach, H. Chadli, A. Rahmani 2016 Trivacancy defects and their effects on the electronic and vibrational properties of single-walled carbon nanotubes, in: 2016 International Renewable and Sustainable Energy Conference (IRSEC), IEEE 50-53 (225) 9
[26] J. Yuan, K. M. Liew 2009 Effects of vacancy defect reconstruction on the elastic properties of carbon nanotubes, Carbon 47 (6) 1526-1533.
[27] M. Sammalkorpi, A. Krasheninnikov, A. Kuronen, K. Nordlund, K. Kaski 2004 Mechanical properties of carbon nanotubes with vacancies and related defects, Physical Review B 70 (24) 245416.
[28] M. Terrones, H. Terrones, F. Banhart, J.-C. Charlier, P. Ajayan 2000 Coalescence of single-walled carbon nanotubes, Science 288 (5469) 1226-1229.
[29] H. He, B. Pan 2008 Electronic structures and vibrational properties of a carbon nanotube with adsorption of small hydrocarbon radicals, The Journal of Physical Chemistry C 112 (48) 18876-18881.
[30] N. Neophytou, S. Ahmed, G. Klimeck 2007 Influence of vacancies on metallic nanotube transport properties, Applied physics letters 90 (18) 182119.
[31] E. Faizabadi 2011 Single wall carbon nanotubes in the presence of vacancies and related energy gaps, in: Electronic Properties of Carbon Nanotubes, IntechOpen.
[32] M. S. Dresselhaus, G. Dresselhaus, R. Saito, A. Jorio 2005 Raman spectroscopy of carbon nanotubes, Physics reports 409 (2) 47-99.
[33] S. Rols, A. Righi, L. Alvarez, E. Anglaret, R. Almairac, C. Journet, P. Bernier, J. Sauvajol, A. Benito, W. Maser, et al. 2000 Diameter distribution of single wall carbon nanotubes in nanobundles, The European Physical Journal B-Condensed Matter and Complex Systems 18 (2) 201-205.
[34] L. Wirtz, A. Rubio 2004 The phonon dispersion of graphite revisited, Solid State Communications 131 (3-4) 141-152.
[35] J. M. Soler, E. Artacho, J. D. Gale, A. Garcia, J. Junquera, P. Ordejon, D. Sanchez-Portal 2002 The siesta method for ab initio order-n materials simulation, Journal of Physics: Condensed Matter 14 (11) 2745.
[36] S. Guha, J. Menendez, J. Page, G. Adams 1996 Empirical bond polarizability model for infullerenes, Physical

Review B 53 (19) 13106.